



Lasers in Manufacturing Conference 2023

# UV nanosecond laser pulse-on-demand operation for high-throughput microstructuring

Jaka Mur<sup>a</sup>, Julien Didierjean<sup>b</sup>, Jernej Jan Kočica<sup>a</sup>, Arnaud Guillosoy<sup>b</sup>, Julien Saby<sup>b</sup>, Jaka Petelin<sup>a</sup>, Alexandra Bourtereau<sup>c</sup>, Girolamo Mincuzzi<sup>c</sup>, Rok Petkovšek<sup>a,\*</sup>

<sup>a</sup>Faculty of Mechanical Engineering, University of Ljubljana, Aškerčeva 6, SI-1000 Ljubljana, Slovenia

<sup>b</sup>Bloom Lasers, Avenue de Canteranne 11, 33600 Pessac, France

<sup>c</sup>ALPhANOV, Aquitania Institute of Optics, Rue François Mitterrand, 33400 Talence, France

---

## Abstract

Industrial UV nanosecond lasers represent a relatively low cost and effective tool for machining a wide variety of materials, from metals to polymers, glass, and transparent dielectrics. Proven industrial applications sparked the ongoing trend to improve the laser stability, reduce the costs, and increase the throughput. The maximal scanner throughput can be achieved by controlling the laser pulse emission through the so-called pulse-on-demand (POD) laser operation. We present a novel POD seeding module jointly utilized with a high-power MHz-level rod-type UV nanosecond laser for microstructuring applications. We studied the effects of scanning speed on POD operation, using state-of-the-art galvanometric scanners, reaching 20 m/s scanning speeds with a 10  $\mu\text{m}$  diameter laser beam. We analysed single- and multi-pass laser percussion drilling performance of metal and polymer materials to assess the setup accuracy and precision, surface structuring of ITO-glass material, and ablation efficiency for pulse durations in range of 1-4 ns.

Keywords: pulse-on-demand; nanosecond pulses; UV laser; microstructuring

---

## 1. Introduction

Laser microstructuring has been widely used in the last decades (Kerse *et al.*, 2016; Mur *et al.*, 2017; Mur and Petkovšek, 2018; Žemaitis *et al.*, 2019; Bonamis *et al.*, 2020), being a versatile and contactless processing method, achieving high precision and structure quality (Indrišiūnas and Gedvilas, 2022). A common method is nanosecond laser ablation due to laser source availability and high process efficiency. Numerous metallic materials exhibit low reflectivity in the ultraviolet (UV) (Amoruso, 1999), making the use of UV advantageous to IR and green pulses (Lasemi *et al.*, 2018; Paeng *et al.*, 2015). UV allows for inherent tighter focusing and smaller heat-affected zone on the surrounding material (Cangueiro *et al.*, 2021; Semerok *et al.*, 1999). UV

---

\* Corresponding author. Tel.: +386 1 4771 615.

E-mail address: rok.petkovsek@fs.uni-lj.si.

nanosecond laser source represent an effective tool for cutting, drilling, engraving, and structuring a variety of materials, in addition to metals also polymers (Wu et al., 2021), glass (Witzendorff et al., 2016; Q. Wang et al., 2020), and transparent dielectrics (Fang et al., 2021). Industrial applications in sectors such as portable electronics (Jourdan et al., 2020), semiconductors (Besaucèle et al., 2019; Y.-R. Wang et al., 2020) sparked the ongoing trend to improve the laser stability, reduce the cost per watt, and increase the throughput (Girolamo Mincuzzi et al., 2020). The latter can be achieved by increasing the pulse energy, the repetition rate, or both, effectively increasing the average laser power. One such example are laser sources based on rod-type fibers (Cha et al., 2021), delivering high-quality UV gaussian beams in ns pulses with a repetition rate in the MHz regime and energies in the of several tens of  $\mu\text{J}$  range.

Final material processing throughput depends on the scanning system as well as the laser source. The fastest scanners, e.g., polygon and resonant, sacrifice flexibility for high-speed linear scanning (Mur et al., 2019). On the other hand, galvo-scanners have limited performance due to mechanical effects and rely on fast acceleration at the beginning of a scanning line and deceleration at its end. At repetition rates in the MHz range, this results in a reduced accuracy and precision in pulse deposition, causing nonhomogeneous structuring or local over-machining. Technological solutions exist, e.g., the scanning strategy called skywriting, as well as research related to its optimization (Jaeggi et al., 2016; G. Mincuzzi et al., 2020), nevertheless causing an increased processing time due to additional scanner motion involved. Maximal scanner throughput is reached by controlling the laser pulse emission through the pulse-on-demand (POD) approach. The POD operation refers to the laser source delivering pulses in sync with an aperiodic external trigger (Černe et al., 2020; Marš et al., 2022; Petelin et al., 2021; Petkovšek et al., 2015; Yokoyama et al., 2014), which is difficult to realize at high repetition rates.

Here we present a novel POD module utilized jointly with a MHz rod type UV nanosecond laser, operating in an intrinsic POD regime, i.e., without an external pulse picker. The laser was coupled with fast galvanometric scanners, achieving scanning speeds up to 20 m/s on material. We evaluated the performance of the setup in terms of precision, accuracy, and ablation efficiency. We studied the effects of scanning speed on POD operation, surface structuring of FTO-glass sandwich materials for precision measurements, and ablation efficiency for pulse durations in range of 1-4 ns.

## 2. Experiment

Experiments were conducted on an open bench processing system built with industrial grade equipment, typical for laser processing. The UV laser beam with 343 nm wavelength was guided to x-y galvo-scanners (ScanLab Excelliscan 14) and focused through a 100 mm f-theta lens, as shown in Fig. 1a. The resulting beam parameters on material surface were: a maximal scan speed of 20 m/s, a calculated  $1/e^2$  laser spot diameter of  $11 \pm 1 \mu\text{m}$ , and a maximal pulse fluence of about  $15 \text{ J/cm}^2$ .

The laser was based on a direct-modulation diode system for seeding, followed by multiple amplifier stages, and final conversion into UV. The POD-enabled seeding stage was custom designed for the experiments and combined with the amplifying stage provided by Bloom Lasers. The UV output laser beam exhibited a high beam quality factor (M-squared parameter  $M^2 < 1.1$ ). The amplifying stage enabled output powers up to 30 W at 400 kHz repetition rate or up to 300  $\mu\text{J}$  pulse energy, while keeping high quality output beam (astigmatism below 8 %, ellipticity below 5 %). For the microstructuring experiments, the output UV nanosecond pulses were set between 1.0 ns and 4.0 ns in duration, with average power reaching around 15 W at a 1.0 MHz repetition rate measured at the laser output, and a corresponding 15  $\mu\text{J}$  pulse energy. The POD operation was facilitated by scan vectors being converted to a train of trigger signals, with time delays corresponding to the desired pulse spacing given the corresponding scanning speed. The whole POD signal for a 15 mm long scanning line is shown in Fig. 1b, with the zoomed-in panel providing a closer look at the beginning. In this

case, a straight scanning line with the target scanning velocity of 20 m/s, the resulting laser output frequency varied from approx. 30 kHz to 1.0 MHz to keep pulse spacing constant, with a temporal resolution of laser output of 5 ns.

Various industrial-standard materials were microstructured, with UV nanosecond pulse energy set to sufficient levels to induce material evaporation and plasma formation, as well as melt ejection. The following materials and approaches were used:

1. Evaluation of POD in comparison with standard and skywriting scanning regimes in terms of structure

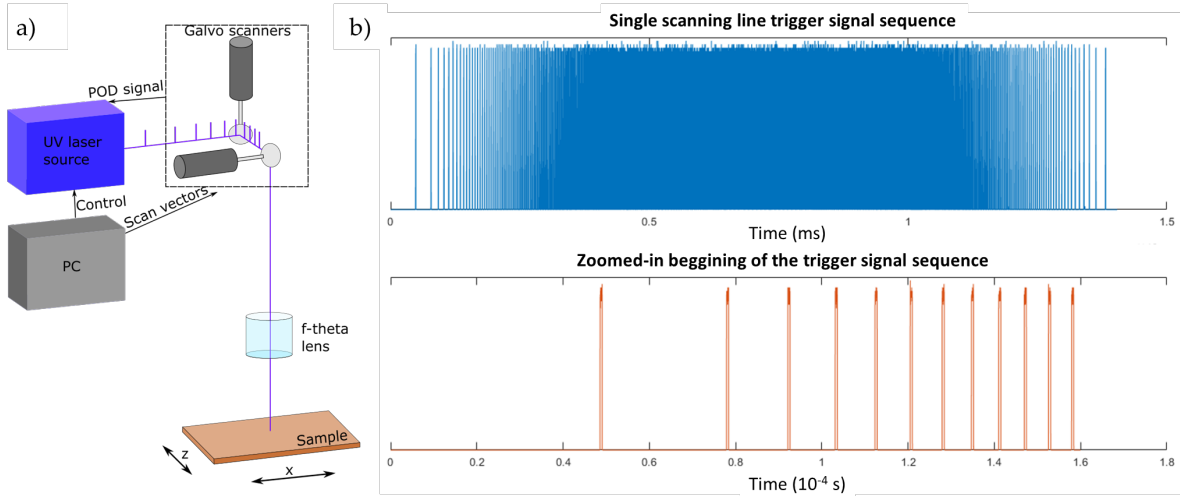


Fig. 1. a) Experimental setup schematics. b) POD sequence received from the galvo scanners, based on scanning a 15 mm long straight line with a maximal velocity of 20 m/s.

quality and precision were carried out on Kapton and polished stainless steel, scanning squares at different scanning speeds and at a fixed pulse-to-pulse distance. The materials were chosen to ensure smooth surface finishes and obtain results on two optically entirely different materials (dielectric and metal, respectively).

2. The accuracy was tested via precision ablation of the ITO layer on glass substrate, comparing the actual ablation crater positioning with the set values at 20 m/s scanning speed.
3. The surface ablation experiments, a microstructuring example, were conducted on polished stainless steel, enabling a comparison of structure depth and ablation efficiency at different pulse durations.

Measurements of resulting structures were carried out using a high magnification optical microscope in both bright field and dark field modes (Olympus BX53M microscope with Olympus MPlanFL 10x, 20x, and 50x objectives). High magnification enabled precise focal plane recognition for measurements of structure depth with high vertical sensitivity. Single craters in the ITO layer were imaged by bright field microscopy and analyzed by a custom Matlab feature recognition script, typically averaging 10-20 craters at each scanner's setting, to obtain the system precision results.

### 3. Results

#### 3.1. Scanning speed effects

The two most common scanning strategies, i.e., conventional scanning without inertial effects compensation and skywriting, are compared to POD-based approach. Fig. 2 presents a direct comparison of structuring quality obtained using different scanning strategies. Isolated ablation craters on a Kapton surface near the corner of a square scanning path were chosen as a representative shape to highlight the key differences between the strategies. The inter-crater distance was fixed at 20  $\mu\text{m}$ , and the scanning speed was increased from 0.25 m/s to 20 m/s, with the lowest speed positioned innermost, and increasing outwards:  $v = \{0.25; 0.50; 0.75; 1.0; 1.5; 2.0; 2.5; 3.0; 5.0; 7.5; 10; 15; 20\}$  m/s.

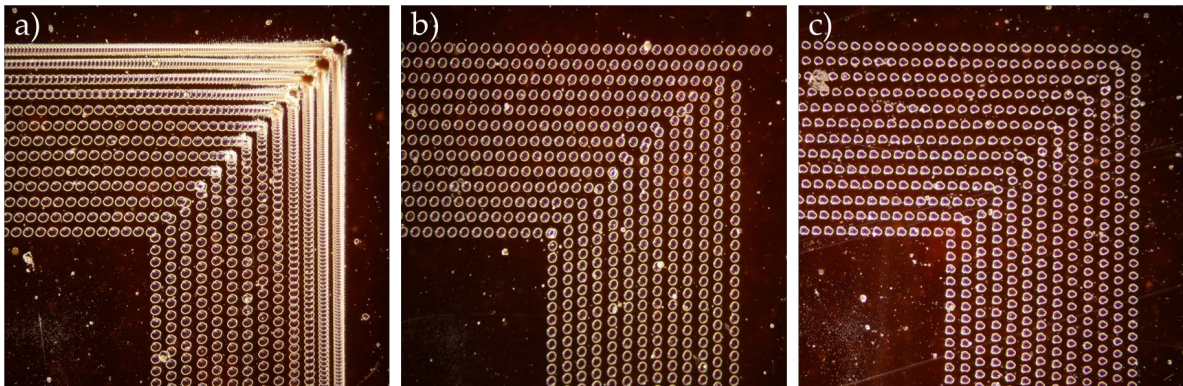


Fig. 2. a) Conventional scanning, b) skywriting, and c) POD. Comparison of scanning strategies by effects in corners of scanning lines using ablation craters in Kapton for a set of different scanning velocities. The scanning speeds used were  $v = \{0.25; 0.50; 0.75; 1.0; 1.5; 2.0; 2.5; 3.0; 5.0; 7.5; 10; 15; 20\}$  m/s, with the lowest speed positioned innermost, and increasing outwards.

The conventional scanning strategy, using fixed laser repetition rate and standard vector scanning, results in evenly spaced craters only for the lowest scanning speed (Fig. 2a,  $v = 0.25$  m/s). At higher scanning speeds a reduction of inter-crater distance is observed during the acceleration/deceleration period of the scanner. Further increasing scanning speeds cause crater accumulation at increasingly long distances from the corner. As the craters start to overlap during the acceleration period, over-machining around the corner is observed.

The use of skywriting makes possible to keep inter-crater distance constant for all scanning speeds, shown in Fig. 2b. Another finding shown in Fig. 2b is that the on/off signals need to be precisely synchronized with scanner motions in order to begin the scanning line at the correct position, and a fixed repetition rate results in positioning jitter of the first pulse in a line. For example, at 20 m/s and 1.0 MHz laser repetition rate, the positioning of the first pulse is only precise to within 20  $\mu\text{m}$ .

The third option, the POD strategy, makes possible to use standard vector scanning and ensure full throughput at undiminished scanning speeds, acceleration, or scanned distances. Inter-crater distances remain constant under all conditions, as shown in Fig. 2c. As the laser repetition rate is constantly adjusted to the scanner motion, the achieved accuracy depends only on the combination of laser timing response and scanner precision.

### 3.2. Positioning accuracy measurement

A stable inter-crater distance is important to successfully execute fast and repetitive scan lines without damaging either the substrate or the surrounding material. To demonstrate the principle, we conducted multi-pass scans on ITO material on glass. Fig. 3a shows isolating lines in ITO, realized with  $N=1-10$  passes at a fixed scanning speed and pulse energy (6.0 m/s and 1.5  $\mu\text{J}$ , respectively). A single pass at the given laser and scanner settings is not enough to selectively remove the entire thickness of the ITO. After two passes, some residual ITO is still present, while 5 and 10 passes result in isolating line of similar width and quality. The isolation properties achieved were tested using a multimeter to measure surface resistivity.

The setup positioning accuracy measurements were based on the average deviation of the measured distance between two successive craters on material from the set value in the galvo-scanner software. The obtained values are shown for different inter-crater distances, including the standard deviation measured over 10-20 crater distances. The scanning speed was kept constant at 20 m/s. The laser repetition rate was set accordingly to achieve set distances from 20  $\mu\text{m}$  to 50  $\mu\text{m}$ , resulting in repetition rates between 1.0 MHz and 400 kHz, respectively. The highest scanning speed corresponds to the worst-case scenario, where the expected precision of the system is at its lowest.

The setup positioning accuracy measurement graph is presented in Fig. 3b, showing the system accuracy in terms of crater position deviation from the set value. It shows no observable trends, either in absolute deviation value or in standard deviation amplitude, with the final accuracy being independent of the inter-crater distance. The measurement itself is influenced by impurities in material, causing a variation in crater shape and size. Nevertheless, the precision of our setup is estimated to be within  $\pm 0.5 \mu\text{m}$  of the target, which is consistent with previously reported data (G. Mincuzzi et al., 2020).

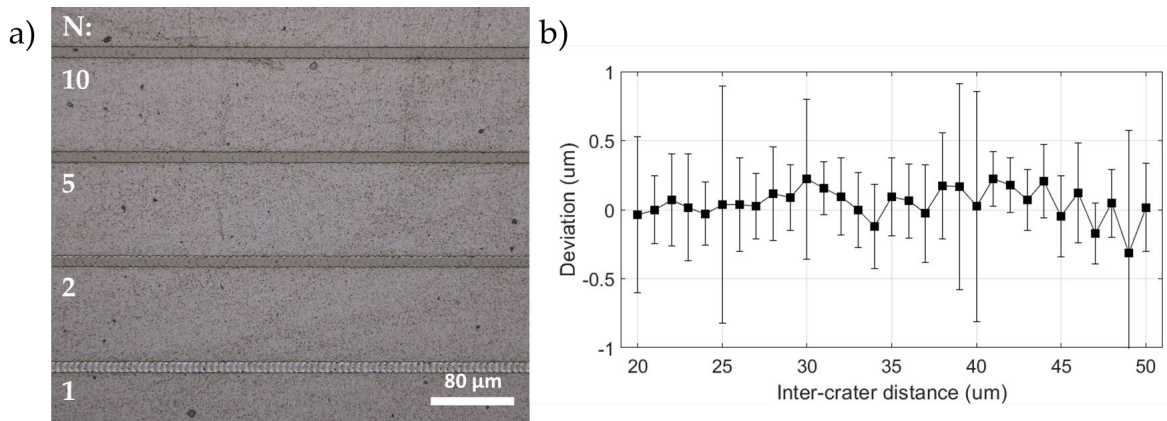


Fig. 3. a) Examples of ITO isolation using multiple high speed scanning passes and an optimized fluence to achieve clean lines with minimal effects on the surrounding material. b) Graph showing the deviation from the expected inter-crater distance at various inter-crater distances and at maximal scanning speed (20 m/s).

### 3.3. Ablation efficiency during microstructuring

Microstructures in stainless steel were chosen for the analysis of ablation depth and efficiency as functions of both the pulse duration and pulse energy. An established approach for microstructuring was used, namely milling, to create relatively large structures in lateral dimension ( $2 \times 2 \text{ mm}^2$ ), to isolate effects of the edges from the surface processing. To obtain measurable structure depths at all pulse energies, the following

structuring parameters were used: 100 repetitions using x-y hatch with 4.0  $\mu\text{m}$  pulse-to-pulse and line-to-line distances.

The graph of optically measured structure depths versus pulse energy for three pulse durations is shown in Fig. 4a. We found that structure depth increases with pulse duration at a given pulse energy and consequently, pulse fluence. As expected, the ablation depth also increases with pulse energy, but at high energies the increase slows, which translates to an ablation efficiency decrease (Fig. 4b). Furthermore, the ablation efficiency graphs for 2 ns and 4 ns pulse durations show a clear peak, suggesting that optimal conversion of laser energy into material removal is achieved in that range. At higher energies, the conversion is less favorable, leading to a higher degree of heat accumulation in the substrate material.

The surface morphology of structure bottoms for different process parameter combinations and a detailed analysis using SEM imaging has been presented in our related work (Kořica et al., 2023).

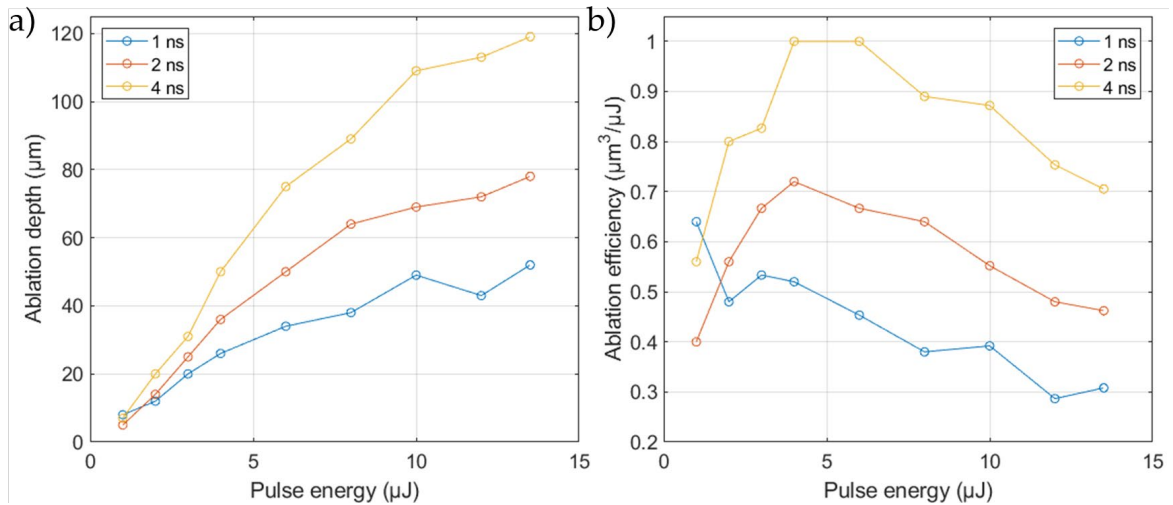


Fig. 4 a) Ablation depth and b) ablation efficiency evolution graphs as a function of the laser pulse energy for three different pulse durations used in the experiment.

#### 4. Conclusion

A first-time demonstration of POD operation in a high-power UV nanosecond laser has been realized and tested on relevant microstructuring applications. First, three different approaches to galvanometric-based scanning were tested and compared, namely skywriting and POD compared to conventional scanning. The results are in line with previously reported work on femtosecond POD technology, showing clear benefits of POD in both throughput and quality.

Further, we evaluated the accuracy and precision of the experimental laser microstructuring setup, by separately measuring the setup accuracy. It is determined by numerous factors, including scanner precision, laser emission timing jitter, sample positioning precision, and other, less predictable effects, such as the response to external vibrations. The remaining factors together contributed to the overall absolute system accuracy to be within  $\pm 0.5 \mu\text{m}$  of the target, consistent with previously reported data.

Lastly, the ablation depth and efficiency were investigated. The research indicates that on stainless steel the use of longer, 4 ns pulses is more efficient compared to shorter 1 ns or 2 ns pulses. Nevertheless, the

resulting surface quality decrease, presented in our related work (Kočica et al., 2023), indicates that this ablation efficiency increase is due to a significantly increased amount of melting and consequent melt ejection.

The POD operation combined with a high-power UV nanosecond laser output is important for applications requiring optimized high throughput, e.g., PCB via drilling, cutting, and de-paneling, or metal surface texturing for batteries, as well as for applications benefiting from a precisely controlled energy distribution on material, e.g., ITO patterning or wafer scribing.

## Acknowledgements

This research was funded by the Slovenian Research Agency - ARRS, grant number P2-0270 and L2-3171.

## References

- Amoruso, S., 1999. Modeling of UV pulsed-laser ablation of metallic targets. *Appl Phys A* 69, 323–332.
- Besaucèle, H., Adnet, A., Beau, F., Bouksou, Y., Bellier, C., Ceccato, P., Chatelain, M., Douri, N., Dusserre, H., Dutems, C., Heintzmann, M., Huet, K., Lenormand, M., Lespinasse, B., Martinez, V., Mazzamuto, F., Melin, A., Perrot, S., Rodrigues, D., Ruet, L., Sannier, O., Thebault, G., Toqué-Tresonne, I., Vestraete, A., Zekri, K., 2019. High energy excimer laser system for nanosecond annealing of semiconductor devices, in: XXII International Symposium on High Power Laser Systems and Applications. Presented at the XXII International Symposium on High Power Laser Systems and Applications, SPIE, pp. 148–153.
- Bonamis, G., Audouard, E., Hönninger, C., Lopez, J., Mishchik, K., Mottay, E., Manek-Hönninger, I., 2020. Systematic study of laser ablation with GHz bursts of femtosecond pulses. *Opt. Express*, OE 28, 27702–27714.
- Canguero, L., Ramos-de-Campos, J.A., Bruneel, D., 2021. Prediction of Thermal Damage upon Ultrafast Laser Ablation of Metals. *Molecules* 26, 6327.
- Černe, L., Petelin, J., Petkovšek, R., 2020. Femtosecond CPA hybrid laser system with pulse-on-demand operation. *Opt. Express*, OE 28, 7875–7888.
- Cha, Y.-H., Kim, S.-W., Shin, J.-H., Kim, J.-M., 2021. Efficient 0.75-mJ 100-kHz ultraviolet pulsed laser based on a rod-type photonic crystal fiber. *Appl. Opt.*, AO 60, 1191–1195.
- Fang, X., Cui, J., Fan, Z., Sun, Z., Mei, X., 2021. Study on Micromachining of Polycrystalline Diamond by UV Nanosecond Laser. *Integrated Ferroelectrics* 219, 28–38.
- Indrišiūnas, S., Gedvilas, M., 2022. Control of the wetting properties of stainless steel by ultrashort laser texturing using multi-parallel beam processing. *Optics & Laser Technology* 153, 108187.
- Jaeggi, B., Neuenschwander, B., Zimmermann, M., Zecherle, M., Boeckler, E.W., 2016. Time-optimized laser micro machining by using a new high dynamic and high precision galvo scanner, in: *Laser Applications in Microelectronic and Optoelectronic Manufacturing (LAMOM) XXI*. Presented at the Laser Applications in Microelectronic and Optoelectronic Manufacturing (LAMOM) XXI, SPIE, pp. 181–191.
- Jourdan, N., Roze, F., Tabata, T., Larivière, S., Contino, A., Mazzamuto, F., Zsolt, T., 2020. UV nanosecond laser annealing for Ru interconnects, in: *2020 IEEE International Interconnect Technology Conference (IITC)*. Presented at the 2020 IEEE International Interconnect Technology Conference (IITC), pp. 163–165.
- Kerse, C., Kalaycıoğlu, H., Elahi, P., Çetin, B., Kesim, D.K., Akçaalan, Ö., Yavaş, S., Aşık, M.D., Öktem, B., Hoogland, H., Holzwarth, R., Ilday, F.Ö., 2016. Ablation-cooled material removal with ultrafast bursts of pulses. *Nature* 537, 84–88.
- Kočica, J.J., Mur, J., Didierjean, J., Guillosoy, A., Saby, J., Petelin, J., Mincuzzi, G., Petkovšek, R., 2023. Pulse-on-Demand Operation for Precise High-Speed UV Laser Microstructuring. *Micromachines* 14, 843.
- Lasemi, N., Pacher, U., Zhigilei, L.V., Bomati-Miguel, O., Lahoz, R., Kautek, W., 2018. Pulsed laser ablation and incubation of nickel, iron and tungsten in liquids and air. *Applied Surface Science* 433, 772–779.
- Marš, M., Petkovšek, R., Agrež, V., 2022. Pump control based pulse on demand operation of frequency doubled Nd:YVO4. *Optics & Laser Technology* 152, 108186.
- Mincuzzi, G., Audouard, E., Bourtereau, A., Delaigue, M., Faucon, M., Hoenninger, C., Mishchik, K., Rebière, A., Sailer, S., Seweryn-Schnur, A., Kling, R., 2020. Pulse to pulse control for highly precise and efficient micromachining with femtosecond lasers. *Opt. Express*, OE 28, 17209–17218.
- Mincuzzi, Girolamo, Rebière, A., Faucon, M., Sikora, A., Kling, R., 2020. Beam engineering strategies for high throughput, precise, micro-cutting by 100 W, femtosecond lasers. *Journal of Laser Applications* 32, 042003.
- Mur, J., Petelin, J., Schille, J., Loeschner, U., Petkovšek, R., 2019. Ultra-fast laser-based surface engineering of conductive thin films.



Applied Surface Science 144911.

- Mur, J., Petkovšek, R., 2018. Precision and resolution in laser direct microstructuring with bursts of picosecond pulses. *Appl. Phys. A* 124, 62.
- Mur, J., Podobnik, B., Poberaj, I., 2017. Laser beam steering approaches for microstructuring of copper layers. *Optics & Laser Technology* 88, 140–146.
- Paeng, D., Yoo, J.-H., Yeo, J., Lee, D., Kim, E., Ko, S.H., Grigoropoulos, C.P., 2015. Low-Cost Facile Fabrication of Flexible Transparent Copper Electrodes by Nanosecond Laser Ablation. *Advanced Materials* 27, 2762–2767.
- Petelin, J., Černe, L., Mur, J., Agrež, V., Kočica, J.J., Schille, J., Loeschner, U., Petkovšek, R., 2021. Pulse-on-demand laser operation from nanosecond to femtosecond pulses and its application for high-speed processing. *Advanced Optical Technologies* 10, 305–314.
- Petkovšek, R., Novak, V., Agrež, V., 2015. High power fiber MOPA based QCW laser delivering pulses with arbitrary duration on demand at high modulation bandwidth. *Opt. Express* 23, 33150–33156. 0
- Semerok, A., Chaléard, C., Detalle, V., Lacour, J.-L., Mauchien, P., Meynadier, P., Nouvellon, C., Sallé, B., Palianov, P., Perdrix, M., Petite, G., 1999. Experimental investigations of laser ablation efficiency of pure metals with femto, pico and nanosecond pulses. *Applied Surface Science* 138–139, 311–314.
- Wang, Q., Zhang, Q., Zhang, Z., Wang, W., Xu, J., 2020. Material removal and surface formation mechanism of C-plane sapphire in multipass ablation by a nanosecond UV laser. *Ceramics International* 46, 21461–21470.
- Wang, Y.-R., Olaizola, S.M., Han, I.S., Jin, C.-Y., Hopkinson, M., 2020. Direct patterning of periodic semiconductor nanostructures using single-pulse nanosecond laser interference. *Opt. Express*, OE 28, 32529–32539.
- Witzendorff, P. von, Bordin, A., Suttman, O., Patel, R.S., Bovatsek, J., Overmeyer, L., 2016. Laser ablation of borosilicate glass with high power shaped UV nanosecond laser pulses, in: *Laser Applications in Microelectronic and Optoelectronic Manufacturing (LAMOM) XXI*. Presented at the Laser Applications in Microelectronic and Optoelectronic Manufacturing (LAMOM) XXI, SPIE, pp. 89–98.
- Wu, C., Rong, Y., Yang, R., 2021. Thermal ablation regulation for ultraviolet (UV) nanosecond laser precision cutting of polycarbonate (PC) film. *Optics & Laser Technology* 143, 107365.
- Yokoyama, Y., Takada, K., Kageyama, T., Tanaka, S., Kondo, H., Kanbe, S., Maeda, Y., Mochida, R., Nishi, K., Yamamoto, T., Takemasa, K., Sugawara, M., Arakawa, Y., 2014. 1064-nm DFB laser diode modules applicable to seeder for pulse-on-demand fiber laser systems. *Optical Fiber Technology, Short Pulse Fiber Lasers* 20, 714–724.
- Žemaitis, A., Gečys, P., Barkauskas, M., Račiukaitis, G., Gedvilas, M., 2019. Highly-efficient laser ablation of copper by bursts of ultrashort tuneable (fs-ps) pulses. *Sci Rep* 9, 1–8.